Inorg. Chem. **2006**, *45*, 10487–10496

Mo(W)/Cu/S Cluster-Based Supramolecular Arrays Assembled from Preformed Clusters $[Et_4N]_4[WS_4Cu_4I_6]$ and $[(n\text{-}Bu)_4N]_2[MoOS_3Cu_3X_3]$ (X = I, SCN) with Flexible Ditopic Ligands

Jian-Ping Lang,*,‡ Qing-Feng Xu,† Wen-Hua Zhang,† Hong-Xi Li,† Zhi-Gang Ren,† Jin-Xiang Chen,† and Yong Zhang†

Key Laboratory of Organic Synthesis of Jiangsu Province, School of Chemistry and Chemical Engineering, Suzhou University, Suzhou 215123, Jiangsu, People's Republic of China, and State Key Laboratory of Organometallic Chemistry, Shanghai Institute of Organic Chemistry, Chinese Academy of Sciences, Shanghai 200032, People's Republic of China

Received June 2, 2006

In our working toward the rational design and synthesis of cluster-based suppramolecular architectures, a set of new $[WS_4Cu_4]$- or $[MoOS_3Cu_3]$-based supramolecular assemblies have been prepared from reactions of preformed cluster compounds $[Et_4N]_4[WS_4Cu_4I_6]$ (**1**) and $[(n\text{-}Bu)_4N]_2[MoOS_3Cu_3X_3]$ (**2**, X = I; **3**, X = SCN) with flexible ditopic ligands such as dipyridylsulfide (dps), dipyridyl disulfide (dpds), and their combinations with dicyanamide (dca) anion and 4,4′-bipy. The cluster precursor **1** reacted with dps or dpds and sodium dicyanamide (dca) in MeCN to produce $[WS_4Cu_4I_2(dps)_3]\cdot 2MeCN$ (**4**·2MeCN) and $[WS_4Cu_4(dca)_2(dpds)_2]\cdot Et_2O\cdot 2MeCN$ (**5**·Et_2O·2MeCN), respectively. On the other hand, treatment of **2** with dpds in DMF/MeCN afforded $[MoOS_3Cu_3I(dpds)_2]\cdot 0.5DMF\cdot 2(MeCN)_{0.5}$ (**6**·0.5DMF·$2(MeCN)_{0.5}$) while reaction of **3** with sodium dicyanamide (dca) and 4,4′-bipy in DMF/MeCN gave rise to $[MoOS_3Cu_3(dca)(4,4'\text{-bipy})_{1.5}]\cdot DMF\cdot MeCN$ (**7**·DMF·MeCN). Compounds **4**·2MeCN, **5**·Et_2O·2MeCN, **6**·0.5DMF·$2(MeCN)_{0.5}$, and **7**·DMF·MeCN have been characterized by elemental analysis, IR spectroscopy, and single-crystal X-ray crystallography. Compound **4** contains a 2D layer array made of the saddle-shaped $[WS_4Cu_4]$ cores interlinked by three pairs of Cu–dps–Cu bridges. Compound **5** has another 2D layer structure in which the $[WS_4Cu_4]$ cores are held together by four pairs of Cu–dca–Cu and Cu–dpds–Cu bridges. Compound **6** displays a 1D spiral chain structure built of the nido-like $[MoOS_3Cu_3]$ cores via two pairs of Cu–dpds–Cu bridges. Compound **7** consists of a 2D staircase network in which each $[MoOS_3Cu_3(4,4'\text{-bipy})]_2$ dimeric unit interconnects with four other equivalent units by a pair of 4,4′-bipy ligands and two pairs of dca anions. The $[WS_4Cu_4]$ core in **4** or **5** and the $[MoS_3Cu_3]$ core in **7** show a planar 4-connecting node and a seesaw-shaped 4-connecting node, respectively, which are unprecedented in cluster-based supramolecular compounds. The successful assembly of **4**–**7** from the three cluster precursors **1**–**3** through flexible ditopic ligands provides new routes to the rational design and construction of complicated cluster-based supramolecular arrays.

Introduction

In the past decades, the modular, topological approach to the rational design and construction of supramolecular arrays has blossomed because the resulting supramolecular compounds are showing very fascinating chemistry and various potential applications in advanced materials.[1−3] Among numerous molecular modules, transition metal clusters have received much attention as structural and functional building blocks for supramolecular assemblies.[4−10] However, because

* To whom correspondence should be addressed. E-mail: jplang@suda.edu.cn.
† Suzhou University.
‡ Shanghai Institute of Organic Chemistry.

(1) (a) Lehn, J.-M. *Supramolecular Chemistry Concepts and Perspectives*; VCH: Weinheim, Germany, 1995; p 139. (b) Stang, P. J.; Olenyuk, B. *Acc. Chem. Res.* **1997**, *30*, 502. (c) Piguet, C.; Bemardinelli, G.; Hopfgartner, G. *Chem. Rev.* **1997**, *97*, 2005. (d) Robson, R. In *Comprehensive Supramolecular Chemistry*; Atwood, J. L., Davies, J. E. D., MacNicol, D. D., Vögtle, F., Lehn, J.-M., Eds.; Pergamon: Oxford, U.K., 1997; Vol. 6, p 733. (e) Yaghi, O. M.; Li, H. L.; Davis, C.; Richardson, D.; Groy, T. L. *Acc. Chem. Res.* **1998**, *31*, 474. (f) Caulder, D. L.; Raymond, K. N. *Acc. Chem. Res.* **1999**, *32*, 975. (g) Swiegers, G. F.; Malefeste, T. J. *Chem. Rev.* **2000**, *100*, 3483. (h) Moulton, B.; Zaworotko, M. J. *Chem. Rev.* **2001**, *101*, 1629. (i) Chisholm, M. H.; Macintosh, A. M. *Chem. Rev.* **2005**, *105*, 2949.

10.1021/ic060974d CCC: $33.50
Published on Web 11/18/2006

Scheme 1

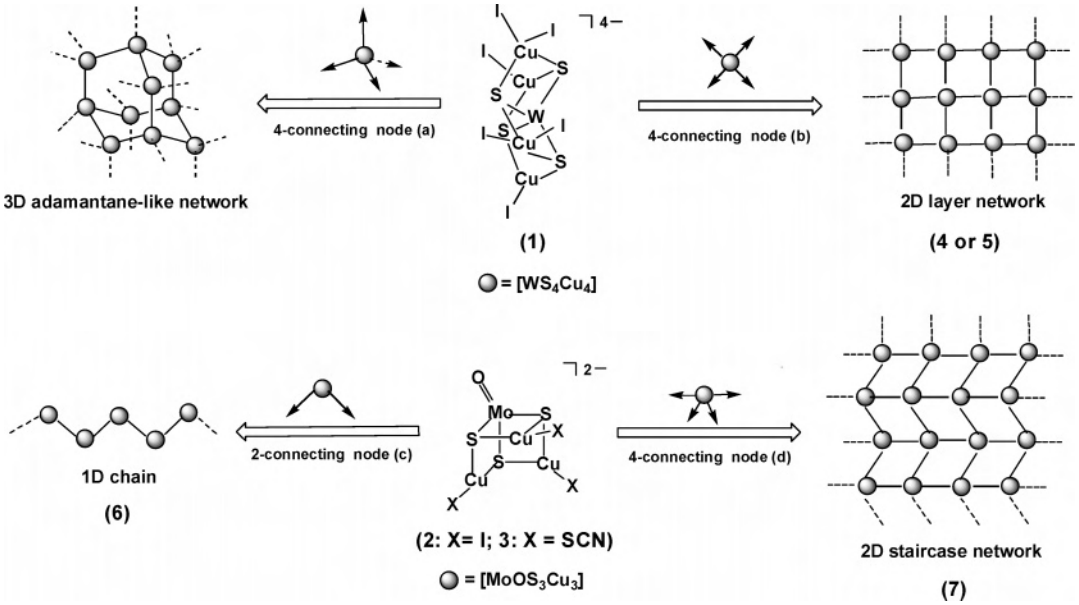

of the limited number of suitable cluster precursors and, especially, the difficulty in the isolation of the resulting assemblies, methodologies to use metal clusters as connecting nodes to hold them together via multitopic ligands in predefined patterns within self-assembled oligomeric or polymeric aggregates still remain a great challenge.

We have recently been interested in the preparation of Mo(W)/Cu/S clusters from thiomolybdate and thiotungstate anions.[11] Some of these clusters, especially those with terminal halides or pseudohalides coordinated at copper(I) centers, may be used as potential building blocks for making multidimensional arrays.[11f,i,j,l] One example was a preformed cluster $[Et_4N]_4[WS_4Cu_4I_6]$[12a] (**1**), in which the saddle-shaped $[WS_4Cu_4]$ core, serving as a tetrahedral 4-connecting node, was connected via 4,4′-bipy ligands to form an intriguing 3D porous polymer $\{[WS_4Cu_4(4,4'\text{-bipy})_4][WS_4Cu_4I_4(4,4\text{-bipy})_2]\}_\infty$.[11i] The other one was $[PPh_4][(\eta^5\text{-}C_5Me_5)WS_3(CuBr)_3]$, in which the incomplete cubanelike $[(\eta^5\text{-}C_5Me_5)WS_3Cu_3]$ core, acting in a 3-connecting node, was linked by bromide and 4,4′-bipy bridges to give rise to a 2D brick-wall polymer $\{[(\eta^5\text{-}C_5Me_5)WS_3Cu_3Br(\mu\text{-}Br)(4,4'\text{-bpy})]\cdot Et_2O\}_\infty$.[11] As an extension of this project, we adopted **1** along with other two incomplete cubanelike analogues $[(n\text{-}Bu)_4N]_2[MoOS_3Cu_3X_3]$ (**2**, X = I;[12b] **3**, X = SCN[12c]) for our further assembly of Mo(W)/Cu/S cluster-based supramolecular compounds.

As shown in Scheme 1, **1** contains a $[WS_4Cu_4]$ core structure in which two Cu atoms have a tetrahedral coordination geometry with two terminal iodides while the other two have a trigonal planar coordination geometry with one terminal iodide. If these iodides are all removed by strong donor ligands, the four copper centers may have up to eight coordination sites available when their coordination geom-

(2) (a) Batten, S. R.; Robson, R. *Angew. Chem., Int. Ed.* **1998**, *37*, 1460. (b) Fujita, M. *Chem. Soc. Rev.* **1998**, *27*, 417. (c) Blake, A. J.; Champness, N. R.; Hubberstey, P.; Li, W. S.; Withersby, M. A.; Schröder, M. *Coord. Chem. Rev.* **1999**, *183*, 117. (d) Hagrman, P. J.; Hagrman, D.; Zubieta, J. *Angew. Chem., Int. Ed.* **1999**, *38*, 2638. (e) Leininger, S.; Olenyuk, B.; Stang, P. J. *Chem. Rev.* **2000**, *100*, 853. (f) Holiday, B. J.; Mirkin, C. A. *Angew. Chem., Int. Ed.* **2001**, *40*, 2022. (g) Seidel, S. R.; Stang, P. J. *Acc. Chem. Res.* **2002**, *35*, 972.

(3) (a) Robson, R.; Hoskins, B. F. *J. Am. Chem. Soc.* **1990**, *112*, 1546. (b) Blake, A. J.; Champness, N. R.; Khlobystov, A. N.; Parsons, S.; Schröder, M. *Angew. Chem., Int. Ed.* **2000**, *39*, 2317. (c) Campos-Femández, C. S.; Clérac, R.; Kooman, J. M.; Russell, D. H.; Dunbar, K. R. *J. Am. Chem. Soc.* **2001**, *123*, 773. (d) Xiong, R. G.; You, X. Z.; Abrahams, B. F.; Xue, Z. L.; Che, C. M. *Angew. Chem., Int. Ed.* **2001**, *40*, 4422. (e) Galan-Mascaros, J. R.; Dunbar, K. R. *Angew. Chem., Int. Ed.* **2003**, *42*, 2289. (f) Berlinguette, C. P.; Dragulescu-Andrast, A.; Sieber, A.; Galan-Mascarós, J. R.; Güdel, H. U.; Achim, C.; Dunbar, K. R. *J. Am. Chem. Soc.* **2004**, *126*, 6222. (g) Jiang, H.; Lin, W. B. *J. Am. Chem. Soc.* **2004**, *126*, 7426. (h) Huang, X. C.; Zhang, J. P.; Chen, X. M. *J. Am. Chem. Soc.* **2004**, *126*, 13218.

(4) (a) Cotton, F. A.; Lin, C.; Murillo, C. A. *Acc. Chem. Res.* **2001**, *34*, 750. (b) Cotton, F. A.; Dikarev, E. V.; Petrukhina, M. A.; Schmitz, M.; Stang, P. J. *Inorg. Chem.* **2002**, *41*, 2903. (c) Cotton, F. A.; Lin, C.; Murillo, C. A. *Inorg. Chem.* **2001,** *40*, 5886. (d) Cotton, F. A.; Lin C.; Murillo, C. A. *Chem. Commun.* **2001**, 11.

(5) (a) Vodak, D. T.; Braun, M. E.; Kim, J.; Eddaoudi, M.; Yaghi, O. M. *Chem. Commun.* **2001**, 2534. (a) Rosi, N. L.; Eckert, J.; Eddaoudi, M.; Vadak, D. T.; Kim, J.; O'Keeffe, M.; Yaghi, O. M. *Science* **2003**, *300*, 1127. (b) Eddaoudi, M.; Moler, D. B.; Li, H. L.; Chen, B.; Reineke, T. M.; O'Keeffe, M.; Yaghi, O. M. *Acc. Chem. Res.* **2001**, *34*, 319.

(6) (a) Ouyang, X.; Campana, C.; Dunbar, K. R. *Inorg. Chem.* **1996**, *35*, 7188. (b) Miyasaka, H.; Campos-Fernández, C. S.; Galán-Mascarós, J. R.; Dunbar, K. R. *Inorg. Chem.* **2000**, *39*, 5870. (c) Miyasaka, H.; Clerac, R.; Campos-Fernandez, C. S.; Dunbar, K. R. *Inorg. Chem.* **2001**, *40*, 1663. (d) Conan, F.; Gall, B. L.; Berbaol, J.-M.; Stang, S. L.; Sala-Pala, J.; Mest, Y. L.; Bacsa, J.; Ouyang, X.; Dunbar, K. R.; Campana, C. F. *Inorg. Chem.* **2004**, *43*, 3673. (e) Chifotides, H. T.; Dunbar, K. R. *Acc. Chem. Res.* **2005**, *38*, 146.

(7) (a) Roland, B. K.; Carter, C.; Zheng, Z. P. *J. Am. Chem. Soc.* **2002**, *124*, 6234. (b) Zheng, Z. P. *Chem. Commun.* **2001**, 2521. (c) Roland, B. K.; Selby, H. D.; Carducci, M. D.; Zheng, Z. P. *J. Am. Chem. Soc.* **2002**, *124*, 3222. (d) Selby, H. D.; Roland, B. K.; Zheng, Z. P. *Acc. Chem. Res.* **2003**, *36*, 935.

(8) (a) Long, J. R.; McCarty, L. S.; Holm, R. H.; J. *Am. Chem. Soc.* **1996**, *118*, 4603. (b) Beauvais, L. G.; Shores, M. P.; Long, J. R. *J. Am. Chem. Soc.* **2000**, *122*, 2763. (c) Bennett, M. V.; Beauvais, L. G.; Shores, M. P.; Long, J. R. *J. Am. Chem. Soc.* **2001**, *123*, 8022. (d) Tulsky, E. G.; Crawford, N. R. M.; Baudron, S. A.; Batail, P.; Long, J. R. *J. Am. Chem. Soc.* **2003**, *125*, 15543.

(9) Abrahams, B. F.; Egan, S. J.; Robson, R. *J. Am. Chem. Soc.* **1999**, *121*, 3535. (b) Abrahams, B. F.; Haywood, M. G.; Robson, R. *Chem. Commun.* **2004**, 938. (c) Yan, B. B.; Zhou, H. J.; Lachgar, A. *Inorg. Chem.* **2003**, *42*, 8818. (d) Yan, Z. H.; Day, C. S.; Lachgar, A. *Inorg. Chem.* **2005**, *44*, 4499.

etries are all made tetrahedral. Therefore, the $[WS_4Cu_4]$ core in **1** is expected to be a complicated multiconnecting node for the ongoing assembly of cluster-based supramolecular frameworks. On the other hand, **2** or **3** may be viewed as having an incomplete cubanelike $[MoOS_3Cu_3]$ core structure in which each Cu atom has a trigonal-planar coordination geometry with a terminal iodide (or thiocyanide). The three copper centers in the cluster core of **2** or **3** may hold up to six coordination sites if these iodides (or thiocyanides) are replaced by strong donor ligands and the coordination geometries of the copper atoms are changed into a tetrahedral one. Topologically, the cluster core in **2** or **3** is also anticipated to serve as an intriguing multiconnecting node.

Previously, we only used rigid linear ditopic donor ligands such as CN^-, 1,4-pyrazine, and 4,4′-bipy to assemble cluster-based supramolecular architectures. As the flexible ditopic ligands were reported to be able to adjust the structures of the target supramolecular compounds,[13−18] we are aware that the connecting nodes of the $[WS_4Cu_4]$ core in **1** and the $[MoOS_3Cu_3]$ core in **2** and **3** may be tuned by some of them into new ones. For instance, the tetrahedral 4-connecting node (a) observed in $\{[WS_4Cu_4(4,4'\text{-bipy})_4][WS_4Cu_4I_4(4,4\text{-bipy})_2]\}_\infty$ may be tuned into a planar 4-connecting node (b) (Scheme 1). Meanwhile, the $[MoOS_3Cu_3]$ core may act as a regular 2-connecting node (c), but may also be changed into a seesaw-type 4-connecting node (d) (Scheme 1). On the basis of the following observations, we have decided to choose two flexible ditopic ligands, dipyridylsulfide (dps) and dipyridyl disulfide (dpds), along with a multidentate ligand, dicyanamide (dca). As indicated in Chart 1, the dps ligand has a cone angle around its central S (dps) (C−S−C = ∼100°) with some flexibility,[16] while the dpds ligand has a twisted structure with C−S−S−C torsion angle of ca. 90° and shows the axial chirality with the *P*- and *M*-forms of enantiomers.[17] The dca ligand has shown extreme coordination versatility.[18] Although these ligands or their combinations with other ligands are always used to make polydimensional complexes, no example has been reported to adopt them for the assembly of cluster-based supramolecular

Chart 1

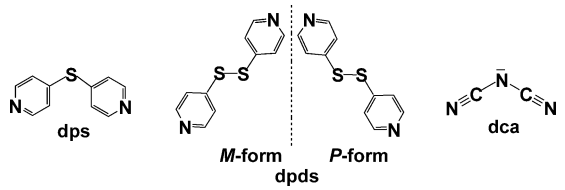

(10) (a) Jin, S.; DiSalvo, F. J. *Chem. Mater.* **2002**, *14*, 3448. (b) Bain, R. L.; Shriver, D. F.; Ellis, D. E. *Inorg. Chim. Acta* **2001**, *325*, 171. (c) Naumov, N. G.; Cordier, S.; Perrin, C. *Angew. Chem., Int. Ed.* **2002**, *41*, 3002. (d) Mironov, Y. V.; Naumov, N. G.; Brylev, K. A.; Efremova, Q. A.; Fedorov, V. E.; Hegetschweiler, K. *Angew. Chem., Int. Ed.* **2004**, *43*, 1297.

(11) (a) Shi, S.; Ji, W.; Tang, S. H.; Lang, J. P.; Xin, X. Q. *J. Am. Chem. Soc.* **1994**, *116*, 3615. (b) Lang, J. P.; Xin X. Q. *J. Solid State Chem.* **1994**, *108*, 118. (c) Lang, J. P.; Kawaguchi, H. Ohnishi, S.; Tatsumi, K. *Chem. Commun*. **1997**, 405. (d) Lang, J. P.; Tatsumi, K. *Inorg. Chem*. **1998**, *37*, 160. (e) Lang, J. P.; Tatsumi, K. *Inorg. Chem*. **1998**, *37*, 6308. (f) Lang, J. P.; Kawaguchi, H.; Tatsumi, K. *Chem. Commun.* **1999**, 2315. (g) Yu, H.; Xu, Q. F.; Sun, Z. R.; Ji, S. J.; Chen, J. X.; Liu, Q.; Lang, J. P.; Tatsumi, K. *Chem. Commun*. **2001**, 2614. (h) Lang, J. P.; Ji, S. J.; Xu, Q. F.; Shen Q.; Tatsumi, K. *Coord. Chem. Rev.* **2003**, *241*, 47. (i) Lang, J. P.; Xu, Q. F.; Chen, Z. N.; Abrahams, B. F. *J. Am. Chem.* Soc. **2003**, *125*, 12682. (j) Lang, J. P.; Xu, Q. F.; Yuan, R. X.; Abrahams, B. F. *Angew. Chem., Int. Ed*. **2004**, *43*, 4741. (k) Lang, J. P.; Jiao, C. M.; Qiao, S. B.; Zhang, W. H.; Abrahams, B. F. *Inorg. Chem*. **2005**, *44*, 2664. (l) Xu, Q. F.; Chen, J. X.; Zhang, W. H.; Ren, Z. G.; Li, H. X.; Zhang, Y.; Lang, J. P. *Inorg. Chem.* **2006**, *45*, 4055.

(12) (a) Lang, J. P.; Bian, G. Q.; Cai, J. H.; Kang, B. S.; Xin, X. Q. *Transition Met. Chem.* **1995**, *20*, 376. (b) Hou, H. W.; Long, D. L.; Xin, X. Q.; Huang, X. Y.; Kang, B. S.; Ge, P.; Ji, W.; Shi, S. *Inorg. Chem.* **1996**, *35*, 5363. (c) Lang, J. P.; Bao, S. A.; Zhu, H. Z.; Xin, X. Q.; Cai, J. H.; Weng, L. H.; Hu, Y. H.; Kang, B. S. *Chem. J. Chin. Univ.* **1992**, *13*, 889.

(13) (a) Fleming, J. S.; Mann, K. L. V.; Carraz, C.; Psillakis, E.; Jeffery, J. C.; McCleverty, J. A.; Ward, M. D. *Angew. Chem., Int. Ed.* **1998**, *37*, 1279. (b) Fujiata, M.; Nagao, S.; Ogura, K. *J. Am. Chem. Soc.* **1995**, *117*, 1649. (c) Seo, J. S.; Whang, D.; Lee, H.; Jun, S. I.; Oh, J.; Jeon, Y. J.; Kim, K. *Nature* **2000**, *404*, 982. (d) Uemura, K.; Kitagawa, S.; Kondo, M.; Fukui, K.; Kitaura, R.; Chang, H. C.; Mizutani, T. *Chem.*—Eur. J. **2002**, *8*, 3586. (e) Pan, L.; Adams, K. M.; Hernandez, H. E.; Wang, X.; Zhang, C.; Hattori, Y.; Kaneko, K. *J. Am. Chem. Soc.* **2003**, *125*, 3062. (f) Kondo, M.; Irie, Y.; Shimizu, Y.; Miyazawa, M.; Kawaguchi, H.; Nakamura, A.; Naito, T.; Maeda, K.; Uchida, F. *Inorg. Chem.* **2004**, *43*, 6139. (g) Carlucci, L.; Ciani, G.; Macchi, P.; Proserpio, D. M.; Rizzato, S. *Chem.*—Eur. J. **1999**, *5*, 237. (h) Reger, D. L.; Semeniuc, R. F.; Rassolov, V.; Smith, M. D. *Inorg. Chem.* **2004**, *43*, 537. (i) Cordes, D. B.; Bailey, A. S.; Caradoc-Davies, P. L.; Gregory, D. H.; Hanton, L. R.; Lee, K.; Spicer, M. D. *Inorg. Chem.* **2005**, *44*, 2544.

(14) (a) Hernández, M. L.; Barandika, M. G.; Urtiaga, M. K.; Cortés, R.; Lezama, L.; Arriortua, M. I.; Rojo, T. *J. Chem. Soc. Dalton. Trans.* **1999**, 1401. (b) van Koningbruggen, P. J.; Garcia, Y.; Kooijman, H.; Spek, A. L.; Haasnoot, J. G.; Kahn, O.; Linares, J.; Codjovi, E.; Varret, F. *J. Chem. Soc., Dalton Trans.* **2001**, 466. (c) Konar, S.; Zangrando, E.; Drew, M. G. B.; Mallah, T.; Ribas, J.; Chaudhuri, N. R. *Inorg. Chem.* **2003**, *42*, 5966. (d) Hennigar, T. L.; Macquarrie, D. C.; Losier, P.; Rogers, R. D. Zaworotko, M. J. *Angew. Chem., Int. Ed. Engl.* **1997**, *36*, 972. (e) Hoskins, B. F.; Robson, R.; Slizys, D. A. *J. Am. Chem. Soc.* **1997**, *119*, 2952. (f) Hoskins, B. F.; Robson, R.; Slizys, D. A. *Angew. Chem., Int. Ed. Engl.* **1997**, *36*, 2236.

(15) (a) Hong, M. C.; Zhao, Y. Y.; Su, W. P.; Cao, R.; Fujita, M.; Zhou, Z. Y.; Chan, A. S. C. *J. Am. Chem. Soc.* **2000**, *122*, 4819. (b) Bu, X. H.; Chen, W.; Lu. S. L.; Zhang, R. H.; Liao, D. Z.; Bu, W. M.; Shionoya, M.; Brisse, F.; Ribas, J. *Angew. Chem., Int. Ed.* **2001**, *40*, 3201. (c) Wu, B. L.; Yuan, D. Q.; Lou, B. Y.; Han, L.; Liu, C. P.; Zhang, C. X.; Hong, M. C. *Inorg. Chem.* **2005**, *44*, 9175. (d) Zou, R. Q.; Liu, C. S.; Huang, Z.; Hu, T. L.; Bu, X. H. *Cryst. Growth* Des. **2006**, *6*, 99. (e) Awaleh, M. O.; Badia, A.; Brisse, F.; Bu, X. H. *Inorg. Chem*. **2006**, *45*, 1560.

(16) (a) Jung, O. S.; Park, S. H.; Kim, D. C.; Kim, K. M. *Inorg. Chem.* **1998**, *37*, 610. (b) Ni, Z.; Vittal, J. J. *Cryst. Growth Des.* **2001**, *1*, 195. (c) Su, X. C.; Zhu, S. R.; Lin, H. K.; Leng, X. B.; Chen, Y. T. *J. Chem. Soc., Dalton Trans.* **2001**, 3163. (d) Muthu, S.; Mi, Z. Vittal, J. J. *Inorg. Chim. Acta* **2005**, *358*, 595.

(17) (a) Tabellion, F. M.; Seidel, S. R.; Arif, A. M.; Stang, P. J. *J. Am. Chem. Soc.* **2001**, *123*, 11982. (b) Blake, A. J.; Brooks, N. R.; Champness, N. R.; Crew, M.; Deveson, A.; Fenske, D.; Gregory, D. H.; Hanton, L. R.; Hubberstey, P.; Schröder, M. *Chem. Commun.* **2001**, 1432. (c) Horikoshi, R.; Mochida, T.; Moriyama, H. *Inorg. Chem.* **2001**, *40*, 2430. (d) Horikoshi, R.; Mochida, T.; Maki, N.; Yamada, S.; Moriyama, H. *J. Chem. Soc., Dalton Trans.* **2002**, 28. (e) Ng, M. T.; Deivaraj, T. C.; Vittal, J. J. *Inorg. Chim. Acta* **2003**, *348*, 173. (f) Ghosh, A. K.; Ghoshal, D.; Lu, T. H.; Mostafa, G.; Ray Chaudhuri, N. *Cryst. Growth Des.* **2004**, *4*, 851. (g) Ng, M. T.; Deivaraj, T. C.; Klooster, W. T.; McIntyre, G. J.; Vittal, J. J. *Chem.*—Eur. J. **2004**, *10*, 5853. (h) Horikoshi, R.; Mochida, T.; Kurihara, M.; Mikuriya, M. *Cryst. Growth Des.* **2005**, *5*, 243.

(18) (a) Yamaochi, H.; Komatsu, T.; Matsukawa, N.; Saito, G.; Mori, T.; Kusunoki, M.; Sakaguchi, *J. Am. Chem. Soc.* **1993**, *115*, 11319. (b) Batten, S. R.; Harris, A. R.; Jensen, P.; Murray, K. S.; Ziebell, A. *J. Chem. Soc., Dalton Trans.* **2000**, 3829. (c) Clerac, R.; Cotton, F. A.; Jeffery, S. P.; Murillo, C. A.; Wang, X. P. *Inorg. Chem.* **2001**, *40*, 1265. (d) Miller, J. S.; Manson, J. L. *Acc. Chem. Res.* **2001**, *34*, 563. (e) Luo, J. H.; Hong, M. C.; Wang, R. H.; Cao, R.; Shi, Q.; Weng, J. B. *Eur. J. Inorg. Chem.* **2003**, 1778. (f) Gao, E. Q.; Bai, S. Q.; Wang, Z. M.; Yan, C. H. *J. Chem. Soc., Dalton Trans.* **2003**, 1759. (g) Zhang, L. Y.; Shi, L. X.; Chen. Z. N. *Inorg. Chem.* **2003**, *42*, 633. (h) Miyasaka, H.; Nakata, K.; Sugiura, K.; Yamashita, M.; Clerac, R. *Angew. Chem., Int. Ed.* **2004**, *43*, 707. (i) Sun, H. L.; Gao, S.; Ma, B. Q.; Su, G.; Batten, S. R. *Cryst. Growth Des.* **2005**, **5**, 269. (j) Sun, H. L.; Wang, Z. M.; Gao, S. *Inorg. Chem.* **2005**, *44*, 2169.

species. With these considerations in mind, we attempted reactions of **1**−**3** with these ligands or their combinations with 4,4′-bipy and obtained four unique $[WS_4Cu_4]$- or $[MoOS_3Cu_3]$-based supramolecular compounds, $[WS_4Cu_4I_2(dps)_3]\cdot 2MeCN$ (**4**·2MeCN), $[WS_4Cu_4(dca)_2(dpds)_2]\cdot Et_2O\cdot 2MeCN$ (**5**·Et_2O·2MeCN), $[MoOS_3Cu_3I(dpds)_2]\cdot 0.5DMF\cdot 2(MeCN)_{0.5}$ (**6**·0.5DMF·$2(MeCN)_{0.5}$), and $[MoOS_3Cu_3(dca)(4,4'\text{-bipy})_{1.5}]\cdot DMF\cdot MeCN$ (**7**·DMF·MeCN). Herein, we report the details on their isolation and structural characterization.

Experimental Section

General Procedures. The cluster precursors **1**−**3** were synthesized by literature methods.[12] Other chemicals and reagents were obtained from commercial sources and used as received. All solvents were predried over activated molecular sieves and refluxed over the appropriate drying agents under argon. The IR spectra were recorded on a Nicolet MagNa-IR 550 as KBr disk (4000−400 cm^{-1}). The elemental analyses for C, H, and N were performed on an EA1110 CHNS elemental analyzer.

$[WS_4Cu_4I_2(dps)_3]\cdot 2MeCN$ (4·2MeCN). To a red solution of $[Et_4N]_4[WS_4Cu_4I_6]$ (37.6 mg, 0.02 mmol) in MeCN (2 mL) was added a solution of dps (11.3 mg, 0.06 mmol) in MeOH (1 mL). The mixture was briefly stirred and filtered. Methanol (10 mL) was carefully layered onto the surface of the filtrate in a glass tube (length = 25 cm, i.d. = 0.6 cm), which was then capped with rubber septum and tightly sealed with Parafilm. The glass tube was left to stand at room temperature for 1 week, forming red prisms of **4**·2MeCN, which were collected by filtration, washed with Et_2O, and dried in air. Yield: 22 mg (75%). Anal. Calcd for $C_{34}H_{30}Cu_4I_2N_8S_7W$: C, 27.84; H, 2.07; N, 7.64. Found: C, 27.56; H, 2.00; N, 7.31. IR (KBr disk): 1615 (m), 1587 (m), 1475 (m), 1410 (m), 1385 (s), 1100 (m), 1058 (m), 809 (m), 716 (m), 447 (m) cm^{-1}.

$[WS_4Cu_4(dca)_2(dpds)_2]\cdot Et_2O\cdot 2MeCN$ (5·Et_2O·2MeCN). To a red solution of $[Et_4N]_4[WS_4Cu_4I_6]$ (37.6 mg, 0.02 mmol) in MeCN (2 mL) was added a solution containing sodium dicyanamide (dca) (7.5 mg, 0.04 mmol) and dpds (8.9 mg, 0.04 mmol) in MeOH (1 mL). Some red precipitate developed quickly. The mixture was stirred for 5 min and filtered. Diethyl ether (10 mL) was carefully layered onto the surface of the filtrate in a glass tube (length = 25 cm, i.d. = 0.6 cm), which was then capped with rubber septum and tightly sealed with Parafilm. The glass tube was left to stand at room temperature for 1 week, forming orange red prisms of **5**·Et_2O·2MeCN, which were collected by filtration, washed with Et_2O, and dried in air. Yield: 16.3 mg (63%). Anal. Calcd for $C_{32}H_{30}Cu_4N_{12}OS_8W$: C, 29.72; H, 2.34; N, 13.00. Found: C, 29.43; H, 2.10; N, 12.65. IR (KBr disk): 2310 (m), 2244 (m), 2164 (s), 1667 (m), 1604 (s), 1532 (m), 1486 (s), 1414 (m), 1386 (s), 1219 (m), 1068 (m), 713 (m), 495 (s), 440 (m) cm^{-1}.

$[MoOS_3Cu_3I(dpds)_2]\cdot 0.5DMF\cdot 2(MeCN)_{0.5}$ (6·0.5DMF·$2(MeCN)_{0.5}$). To a dark red solution of $[n\text{-}Bu_4N]_2[MoOS_3Cu_3I_3]$ (26.6 mg, 0.021 mmol) in 4 mL of DMF/MeCN (v/v = 1:2) was added dpds (9.5 mg, 0.043 mmol). The mixture was stirred for 5 min and then filtered. Slow evaporation of the solvents from the filtrate afforded red plates of **6**·0.5DMF·$2(MeCN)_{0.5}$ several days later, which were collected by filtration, washed with MeCN/Et_2O (v/v = 1: 5), and dried in air. Yield: 14.1 mg (64.3%). Anal. Calcd for $C_{23.5}H_{22.5}Cu_3IMoN_{5.5}O_{1.5}S_7$: C, 27.04; H, 2.18; N, 7.38. Found: C, 26.84; H, 2.11; N. 7.01. IR (KBr disk): 1616 (s), 1585 (s), 1477 (m), 1412 (m), 1385 (s), 1107 (m), 1060 (m), 914 (s), 810 (m), 717 (m), 493 (s), 447 (m) cm^{-1}.

$[MoOS_3Cu_3(dca)(4,4'\text{-bipy})_{1.5}]\cdot DMF\cdot MeCN$ (7·DMF·MeCN). To a dark red solution of $[n\text{-}Bu_4N]_2[MoOS_3Cu_3(NCS)_3]$ (21.2 mg, 0.02 mmol) in 4 mL of DMF/MeCN (v/v = 1:2) was added a solution containing sodium dicyanamide (dca) (1.8 mg, 0.02 mmol) and 4,4′-bipy (6.2 mg, 0.04 mmol) in MeOH (1 mL). Some brown precipitate developed immediately. The resulting mixture was briefly stirred and filtered. A workup similar to that used in the isolation of **6** produced red prisms of **7**·DMF·MeCN. Yield: 8.1 mg (50%). Anal. Calcd for $C_{22}H_{22}Cu_3MoN_8O_2S_3$: C, 32.49; H, 2.73; N, 13.78. Found: C, 32.12; H, 2.64; N, 13.41. IR (KBr disk): 2309 (m), 2250 (m), 2155 (s), 1667 (m), 1604 (s), 1532 (m), 1485 (s), 1412 (s), 1381 (s), 1219 (m), 1068 (m), 910 (s), 713 (m), 446(m) cm^{-1}.

X-ray Data Collection and Structure Determination. X-ray-quality crystals of the compounds were obtained directly from the above preparations. All measurements were made on a Rigaku Mercury CCD X-ray diffractometer by using graphite-monochromated Mo Kα (λ = 0.710 70 Å). Crystals of **4**·2MeCN, **5**·Et_2O·2MeCN, **6**·0.5DMF·$2(MeCN)_{0.5}$, and **7**·DMF·MeCN were mounted with grease at the top of a glass fiber and cooled at 193 K in a liquid-nitrogen stream. Cell parameters were refined by using the program CrystalClear (Rigaku and MSC, ver 1.3, 2001). The collected data were reduced by using the program CrystalClear (Rigaku and MSC, ver 3.60, 2004) while an absorption correction (multiscan) was applied. The reflection data were also corrected for Lorentz and polarization effects.

The crystal structures of **4**·2MeCN, **5**·Et_2O·2MeCN, **6**·0.5DMF·$2(MeCN)_{0.5}$, and **7**·DMF·MeCN were solved by direct methods and refined on F^2 by full-matrix least-squares methods with the SHELXTL-97 program.[19] In the case of **6**·0.5DMF·$2(MeCN)_{0.5}$, the C, N, and O atoms of the three solvated molecules were refined with an occupancy factor of 50%. All non-hydrogen atoms, apart from the C and N atoms of one MeCN solvent molecule bearing N4 in **4**·2MeCN, the C and O atoms of one Et_2O solvent molecule in **5**·Et_2O·2MeCN, and the C and N atoms of one MeCN solvent molecule bearing N8 in **7**·DMF·MeCN, were refined anisotropically. All hydrogen atoms were placed in geometrically idealized positions (C−H = 0.98 Å for methyl groups; C−H = 0.95 Å for phenyl groups) and constrained to ride on their parent atoms with $U_{iso}(H) = 1.2U_{eq}(C)$ for phenyl groups and $U_{iso}(H) = 1.5U_{eq}(C)$ for methyl groups. In the final Fourier maps, the largest electron-density peaks in **4**·2MeCN (2.402 e/Å^3), in **5**·Et_2O·2MeCN (2.166 e/Å^3), in **6**·0.5DMF·$2(MeCN)_{0.5}$ (1.839 e/Å^3), and in **7**·DMF·MeCN (1.195 e/Å^3) were located 1.033 Å from atom W1 in **4**·2MeCN, 1.145 Å from atom W1 in **5**·Et_2O·2MeCN, 1.120 Å from atom Mo1 in **6**·0.5DMF·$2(MeCN)_{0.5}$, and 0.818(1) Å from atom Mo1 in **7**·DMF·MeCN, respectively. A summary of the key crystallographic information for **4**·2MeCN, **5**·Et_2O·2MeCN, **6**·0.5DMF·$2(MeCN)_{0.5}$, and **7**·DMF·MeCN is given in Table 1.

Results and Discussion

Synthesis and Spectral Aspects. Reactions of an acetonitrile solution of **1** with 3 equiv of dps generated a red solution. Diffusion of methanol into this solution formed red prisms of **4**·2MeCN in 75% yield (Scheme 2). However, when an acentonitrile solution of **1** was treated with a methanol solution of 4 equiv of sodium dicyanamide, a large amount of insoluble brown red precipitate was observed to develop within seconds, which excluded the growth of any

(19) Sheldrick, G. M. *SHELXS-97, Program for X-ray Crystal Structure Solution*; University of Göettingen: Göettingen, Germany, 1997.

Table 1. Crystallographic Data for **4**·2MeCN, **5**·Et_2O·2MeCN, **6**·0.5DMF·2$(MeCN)_{0.5}$, and **7**·DMF·MeCN

param	**4**·2MeCN	**5**·Et_2O·2MeCN
molecular formula	$C_{34}H_{30}Cu_4I_2N_8S_7W$	$C_{32}H_{30}Cu_4N_{12}OS_8W$
fw	1466.89	1293.17
cryst system	orthorhombic	orthorhombic
space group	*Ccc*2	$C222_1$
size (mm^3)	0.30 × 0.05 × 0.05	0.30 × 0.15 × 0.10
a (Å)	14.4181(13)	16.396(2)
b (Å)	26.731(3)	17.135(2)
c (Å)	12.6362(12)	18.341(3)
V ($Å^3$)	4870.2(8)	5152.8(12)
Z	4	4
T/K	193	193
D_{calc} (g cm^{-3})	2.001	1.667
?λ(Mo Kα) (Å)	0.710 70	0.710 70
μ (cm^{-1})	56.73	42.10
$2\theta_{max}$ (deg)	50.70	54.96
tot. reflcns	23 493	25 841
unique reflcns	4227 (R_{int} = 0.0671)	5898 (R_{int} = 0.0781)
no. observns	3703 ($I > 2.00\sigma(I)$)	5608 ($I > 2.00\sigma(I)$)
no. params	240	234
R[a]	0.0529	0.0811
wR[b]	0.1311	0.1911
GOF[c]	1.117	1.192
$\Delta\rho_{max}$ (e $Å^{-3}$)	2.402	2.166
$\Delta\rho_{min}$ (e $Å^{-3}$)	−0.891	−1.428

param	**6**·0.5DMF·2$(MeCN)_{0.5}$	**7**·DMF·MeCN
molecular formula	$C_{23.5}H_{22.5}Cu_3IMoN_{5.5}O_{1.5}S_7$	$C_{22}H_{22}Cu_3MoN_8O_2S_3$
fw	1043.85	813.22
cryst system	monoclinic	triclinic
space group	$P2_1/c$	$P\bar{1}$
size (mm^3)	0.35 × 0.28 × 0.08	0.20 × 0.15 × 0.10
a (Å)	10.492(2)	9.2794(19)
b (Å)	20.017(4)	11.063(2)
c (Å)	19.537(4)	15.852(3)
α (deg)	95.68(3)	
β (deg)	90.97(3)	94.28(3)
γ (deg)	114.64(3)	
V ($Å^3$)	4102.7(14)	1459.8(6)
Z	4	2
T/K	193	193
D_{calc} (g cm^{-3})	1.816	1.850
λ(Mo Kα) (Å)	0.710 70	0.710 70
μ (cm^{-1})	29.76	28.26
$2\theta_{max}$ (deg)	50.06	54.96
tot. reflcns	37094	16615
unique reflcns	7150 (R_{int} = 0.060)	6574 (R_{int} = 0.0487)
no. observns	6910 ($I > 2.00\sigma(I)$)	5383 ($I > 2.00\sigma(I)$)
no. params	401	339
R[a]	0.0837	0.0718
wR[b]	0.1980	0.1315
GOF[c]	1.308	1.159
$\Delta\rho_{max}$ (e $Å^{-3}$)	1.839	1.195
$\Delta\rho_{min}$ (e $Å^{-3}$)	−1.415	−0.648

[a] $R = \Sigma||F_o| - |F_c|/\Sigma|F_o|$. [b] $wR = \{\Sigma w(F_o^2 - F_c^2)^2/\Sigma w(F_o^2)^2\}^{1/2}$. [c] GOF = $\{\Sigma[w((F_o^2 - F_c^2)^2)/(n - p)\}^{1/2}$, where n = number of reflections and p = total numbers of parameters refined.

Scheme 2

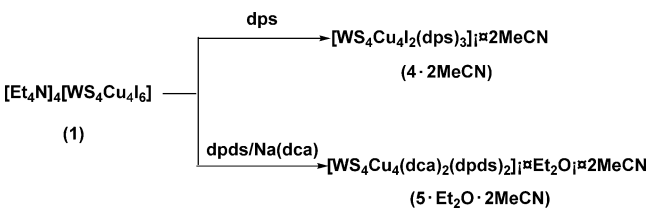

crystals of the resulting products. The solid was washed thoroughly with water, MeCN, MeOH, and Et_2O and dried in vacuo; the composition of this solid was tentatively assumed to be $[WS_4Cu_4(dca)_2]$ by its elemental analysis, IR spectroscopy, and X-ray fluorescence analysis (see Supporting Information). It may be understandable that such a "carbon-deficient" ligand (dca) linked the $[WS_4Cu_4]$ core of **1** to form products with very low solubility in common organic solvents. Therefore, we decided to use a "carbon-rich" flexible ditopic linker, dpds, as a coligand to increase the solubility of the products. Fortunately, reactions of **1** in MeCN with a methanol solution containing 2 equiv of sodium dicyanamide and 2 equiv of dpds gave rise to a red solution coupled with some amount of brown red precipitate. Filtration followed by diffusion of diethyl ether into the filtrate afforded orange red prisms of **5**·Et_2O·2MeCN in 63% yield (Scheme 2).

Scheme 3

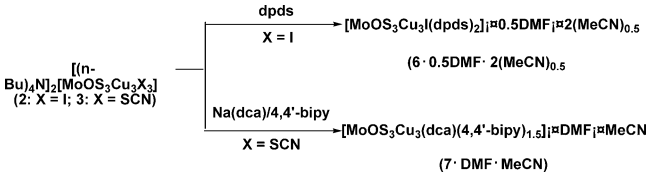

On the other hand, treatment of a solution of **2** in DMF/MeCN (1:2 v/v) with 2 equiv of dpds led to a red solution, from which red plates of **6**·0.5DMF·2$(MeCN)_{0.5}$ were isolated in 64.3% yield (Scheme 3). Addition of a methanol solution of equimolar sodium dicyanamide into a solution of **3** in DMF/MeCN (1:2 v/v) always yielded a large amount of an insoluble brown precipitate within seconds. To increase the solubility of the products, we attempted many combinations of dca with ditopic ligands such as dps, dpds, and 4,4′-bipy. Fortunately, reactions of **3** in DMF/MeCN with a methanol solution containing equimolar sodium dicyanamide and 2 equiv of 4,4′-bipy gave rise to a red solution coupled with some amount of brown precipitate. Filtration followed by a workup similar to that used in the isolation of **6** afforded red prisms of **7**·DMF·MeCN in 50% yield (Scheme 3).

Solids **4**−**7** were relatively stable toward air and moisture and were slightly insoluble in DMF and DMSO. The elemental analysis was consistent with the chemical formula of **4**−**7**. In the IR spectra of **5** and **7**, bands at 2310/2244/2164 (**5**) or 2309/2250/2155 (**7**) cm^{-1} were assigned to be the stretching vibrations of the dca ligand with a bidentate $\mu_{1,5}$ coordination.[6c] For **5** and **6**, the peak at 495 cm^{-1} in **5** or 493 cm^{-1} in **6** was assigned to be the S−S stretching vibration of the dpds ligand.[17g] In addition, the IR spectra of **4** and **5** showed the bridging W−S stretching vibrations at 447 (**4**) and 440 (**5**) cm^{-1} while **6** and **7** showed one terminal Mo═O and one bridging Mo−S stretching vibrations at 914/447 cm^{-1} (**6**) and 910/446 (**7**) cm^{-1}. The identities of **4**−**7** were further confirmed by X-ray crystallography.

Crystal Structure of $[WS_4Cu_4I_2(dps)_3]$·2MeCN (4·2MeCN). Complex **4**·2MeCN crystallized in the orthorhombic space group *Ccc*2, and the asymmetric unit contains half of the $[WS_4Cu_4I_2(dps)_3]$ molecule and two MeCN-solvated molecules. Figure 1 shows the perspective view of the repeating unit of **4**, and Table 2 lists the selected bond lengths and angles for **4**. The tungsten and copper centers in **4** kept

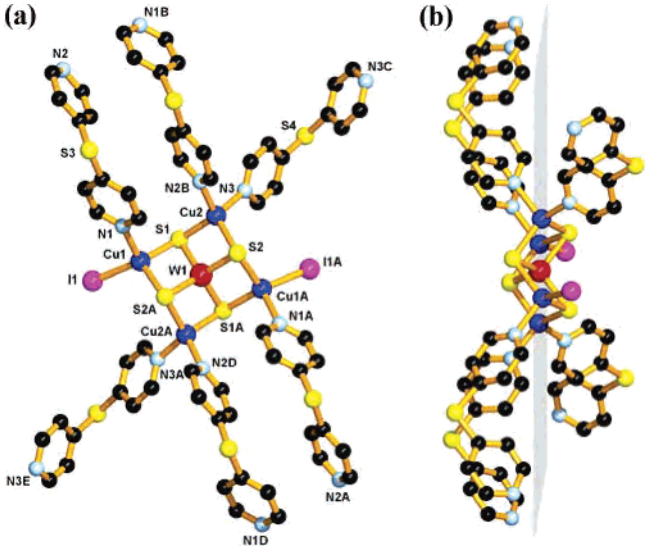

Figure 1. (a) Perspective view of the repeating unit of **4** with 50% thermal ellipsoids. All hydrogen atoms are omitted for clarity. Symmetry transformations used to generate equivalent atoms: (A) $-x + 1, -y + 1, z$; (B) $-x, -y + 1, z$; (C) $-x + 0.5, -y + 0.5, z$; (D) $x + 1, y, z$; (E) $x + 0.5, y + 0.5, z$. (b) Side view of the repeating unit of **4**.

Table 2. Selected Bond Distances (Å) and Angles (deg) for **4**

W1−S1	2.234(3)	W1−S1A	2.234(3)
W1−S2	2.238(3)	W1−S2A	2.238(3)
W1−Cu2	2.6736(12)	W1−Cu2A	2.6736(13)
W1−Cu1A	2.7129(13)	W1−Cu1	2.7129(13)
I1−Cu1	2.5661(19)	Cu1−N1	2.117(11)
Cu1−S2A	2.293(4)	Cu1−S1	2.314(4)
Cu2−N3	2.054(10)	Cu2−N2B	2.072(12)
Cu2−S2	2.291(4)	Cu2−S1	2.307(4)
S2−Cu1A	2.293(4)	N2−Cu2F	2.072(12)
S1−W1−S1A	109.0(2)	S1−W1−S2	109.96(12)
S1A−W1−S2	108.88(12)	S1−W1−S2A	108.88(12)
S1A−W1−S2A	109.96(12)	S2−W1−S2A	110.15(19)
Cu2−W1−Cu2A	179.52(10)	Cu2−W1−Cu1A	88.41(4)
Cu2A−W1−Cu1A	91.58(4)	Cu2−W1−Cu1	91.58(4)
Cu2A−W1−Cu1	88.41(4)	Cu1A−W1−Cu1	178.01(9)
N1−Cu1−S2A	108.6(3)	N1−Cu1−S1	106.0(3)
S2A−Cu1−S1	104.31(12)	N1−Cu1−I1	103.2(3)
S2A−Cu1−I1	115.82(10)	S1−Cu1−I1	118.24(13)
N3−Cu2−N2B	99.9(4)	N3−Cu2−S2	118.3(3)
N2B−Cu2−S2	108.5(3)	N3−Cu2−S1	109.6(3)
N2B−Cu2−S1	115.3(3)	S2−Cu2−S1	105.57(12)
W1−S1−Cu2	72.12(11)	W1−S1−Cu1	73.23(10)
Cu2−S1−Cu1	113.35(17)	W1−S2−Cu2	72.35(10)
W1−S2−Cu1A	73.55(11)	Cu2−S2−Cu1A	110.04(17)
C8−S3−C3	103.5(7)	C13−S4−C13C	101.3(9)

their +6 and +1 oxidation states in **1**. The $[WS_4Cu_4I_2(dps)_3]$ molecule consists of the saddle-shaped $[WS_4Cu_4]$ core structure similar to that of **1**. W1 atom is located at a 2-fold axis while S4 atom is lying at another 2-fold axis. All four copper centers in **4** adopt a distorted tetrahedral coordination geometry, coordinated by two μ_3-S atoms from the $[WS_4]^{2-}$ anion and two N atoms from two dps ligands or two iodine atoms. The W1···Cu1 contact is longer than the W1···Cu2 contact. Their mean value (2.6933(13) Å) is close to the corresponding one in **1** (2.686(1) Å) and $\{[WS_4Cu_4(4,4'\text{-bipy})_4][WS_4Cu_4I_4(4,4\text{-bipy})_2]\}_\infty$ (2.689(2) Å)[11i] but shorter than those in clusters containing tetrahedrally coordinated Cu such as $[WS_4Cu_4(dppm)_4](PF_6)_2$ (2.760(1) Å)[11e] and $[(\eta^5\text{-}C_5Me_5)WS_3Cu]_4$ (2.751(3) Å).[20a] The average Cu−μ_3-S bond length (2.301(4) Å) is slightly shorter than those

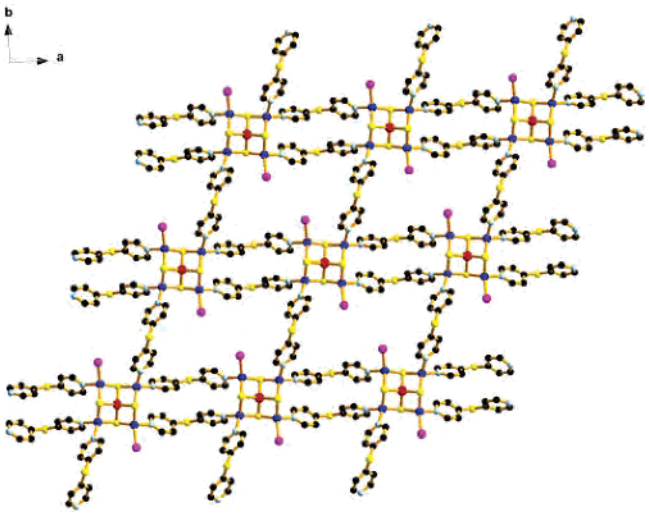

Figure 2. Extended structure of **4** looking down the *c* axis.

reported in other tetrahedrally coordinated Cu clusters such as **1** (2.316(4) Å) and $[WS_4Cu_4(dppm)_4](PF_6)_2$ (2.351(3) Å). The terminal Cu1−I1 length of 2.5661(19) Å is between that in **1** (average 2.540(3) Å) and that of $\{[WS_4Cu_4(4,4'\text{-bipy})_4][WS_4Cu_4I_4(4,4\text{-bipy})_2]\}_\infty$ (2.571(2) Å). The mean Cu−N length (2.081(11) Å) and W1−μ_3-S distance (2.236(3) Å) are normal. The C−S−C angles of the dps ligands are in the range of 101.3(9)−103.5(7)°, which is comparable to those found in $[Cu(dps)_2](ClO_4)$ (103.6(4)−103.8(4)°).[16b]

From a topological perspective, the saddle-shaped $[WS_4Cu_4]$ core in **4** acts as a 4-connecting node, which is remarkably different from the tetrahedral 4-connecting one observed in $\{[WS_4Cu_4(4,4'\text{-bipy})_4][WS_4Cu_4I_4(4,4\text{-bipy})_2]\}_\infty$. In **4**, the six flexible dsp ligands are surrounding the $[WS_4Cu_4]$ core in a way that the mean deviation from the least-squares plane consisting of N2, N1B, N3C, N2A, N1D, and N3E atoms is ca. 1.16 Å. This suggests that the six coordination sites of the six dps ligands are approximately lying on the plane highlighted in gray in Figure 1b. Thus, the $[WS_4Cu_4]$ core in **6** under the presence of the six dps ligands may be viewed as a planar 4-connecting node, which is unprecedented in the cluster-based supramolecular chemistry. Such a 4-connecting node no doubt prefers to generate a two-dimensional network. Therefore, each $[WS_4Cu_4]$ core in **4** is interlinked by a pair of dps ligands to form a 1D $[WS_4Cu_4I_2(dps)_2]_n$ linear chain extended along the *a* axis. Such a chain is further interconnected via dps ligands to form a 2D layer structure with a parallelogrammic mesh that extends along the *ab* plane (Figure 2). The MeCN solvent molecules are lying between layers, and there is no evident interaction between the layers and/or the solvated molecules.

Crystal Structure of $[WS_4Cu_4(dca)_2(dpds)_2]\cdot Et_2O\cdot 2MeCN$ ($5\cdot Et_2O\cdot 2MeCN$). Compound $5\cdot Et_2O\cdot 2MeCN$ crystallizes in the orthorhombic space group $C222_1$, and the asymmetric unit contains half of the $[WS_4Cu_4(dca)_2(dpds)_2]$ molecule, half of Et_2O, and two MeCN-solvated molecules. Figure 3 depicts the perspective view of the repeating unit of **5**, and Table 3 presents the selected bond lengths and

(20) Lang, J. P.; Tatsumi, K. *J. Organomet. Chem.* **1999**, *579*, 332.

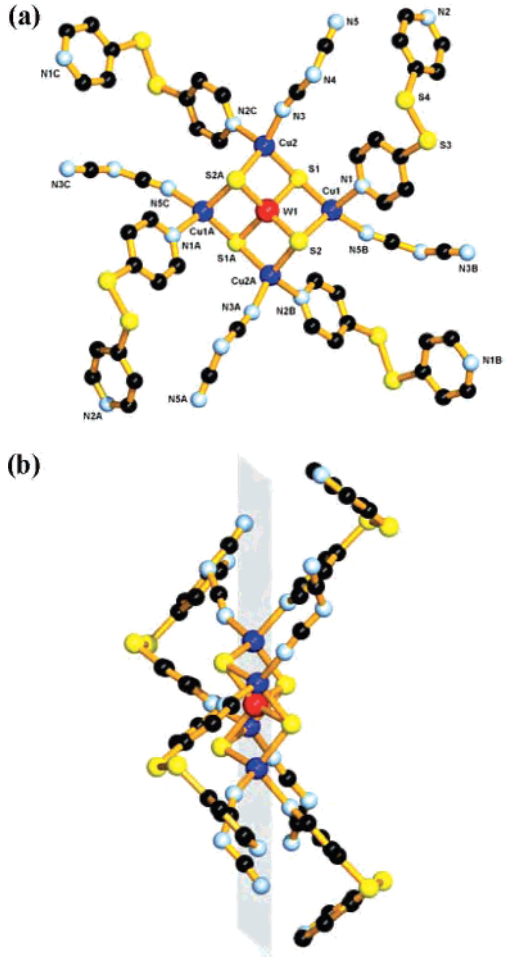

Figure 3. (a) Perspective view of the repeating unit of **5** with 50% thermal ellipsoids. All hydrogen atoms are omitted for clarity. Symmetry transformations used to generate equivalent atoms: (A) x, $-y+2$, $-z+1$; (B) $-x+1.5$, $y-0.5$, $-z+1.5$; (C) $-x+1.5$, $-y+2.5$, $z-0.5$. (b) Side view of the repeating unit of **5**.

Table 3. Selected Bond Distances (Å) and Angles (deg) for **5**

W1−S2	2.224(3)	W1−S2A	2.224(3)
W1−S1	2.242(3)	W1−S1A	2.242(3)
W1−Cu1	2.6717(14)	W1−Cu1A	2.6717(14)
W1−Cu2A	2.7015(15)	W1−Cu2	2.7015(15)
Cu1−N5B	1.994(14)	Cu1−N1	2.089(11)
Cu1−S1	2.283(4)	Cu1−S2	2.292(4)
Cu2−N3	1.972(11)	Cu2−N2C	2.099(11)
Cu2−S2A	2.292(3)	Cu2−S1	2.301(4)
S3−S4	2.035(6)		
S2−W1−S2A	109.78(18)	S2−W1−S1	109.44(12)
S2−W1−S1A	108.86(12)	S2A−W1−S1	108.86(12)
S2A−W1−S1A	109.44(12)	S1−W1−S1A	110.4(2)
Cu1−W1−Cu1A	179.33(9)	Cu1−W1−Cu2A	88.03(5)
Cu1A−W1−Cu2A	91.95(5)	Cu1−W1−Cu2	91.95(5)
Cu1A−W1−Cu2	88.03(5)	Cu2A−W1−Cu2	176.73(8)
N5B−Cu1−N1	96.3(5)	N5B−Cu1−S1	116.0(5)
N1−Cu1−S1	116.4(3)	N5B−Cu1−S2	116.1(5)
N1−Cu1−S2	106.3(3)	S1−Cu1−S2	105.67(12)
N3−Cu2−N2C	102.6(4)	N3−Cu2−S2A	112.9(4)
N2C−Cu2−S2A	109.8(3)	N3−Cu2−S1	119.6(4)
N2C−Cu2−S1	107.1(3)	S2A−Cu2−S1	104.55(13)
W1−S1−Cu1	72.36(11)	W1−S1−Cu2	72.96(11)
Cu1−S1−Cu2	114.90(16)	W1−S2−Cu2A	73.45(11)
W1−S2−Cu1	72.51(10)	Cu2A−S2−Cu1	109.04(15)

angles for **5**. The $[WS_4Cu_4]$ unit in **5** again retains the core structure of **1**. The central W1 atom is lying on a 2-fold axis. Each copper center also adopts a distorted tetrahedral coordination geometry, coordinated by two μ_3-S atoms and two N atoms from dca anion and dpds liagnd. The mean W1···Cu, Cu−μ_3-S, and W−μ_3-S bond lengths are quite similar to those of the corresponding ones of **4**. The mean Cu−N(dpds) bond length (2.094(11) Å) is close to that of **4**. Each dca ligand acts as a normal $\mu_{1,5}$ coordination mode. The mean Cu−N(dca) bond length (1.983(14) Å) is similar to those observed in $[Cu_4(4,4'\text{-bipy})_4(dca)_4(MeCN)_2]$ (1.964(4) Å) and $[Cu_6(dca)_6(bipye)_6]$ (1.971(3) Å; bipye = bis(4-pyridyl)ethene).[18b] The gauche conformation of each dtdp ligand in **5** is basically retained relative to that of the free dtds ligand.[17a] Its S−S bond length (2.035(6) Å) is comparable to that of the free ligand (2.03 Å) and those reported in metal/dpds complexes such as $[(Et_3P)_2Pt(dpds)]_2(NO_3)_4$ (2.03(3) Å)[17a] and $[Cu(hfac)_2(dpds)]$ (2.029(3) Å, hfac = 1,1,1,5,5,5-hexafluoroacetylacetonate).[17c] Meanwhile, its C−S−S−C dihedral angle (84.3°) is almost the same as that of the free dpds ligand (84°) but smaller than those of $[(Et_3P)_2Pt(dpds)]_2(NO_3)_4$ (91.6°) and $[Cu(hfac)_2(dpds)]$ (88.1°).

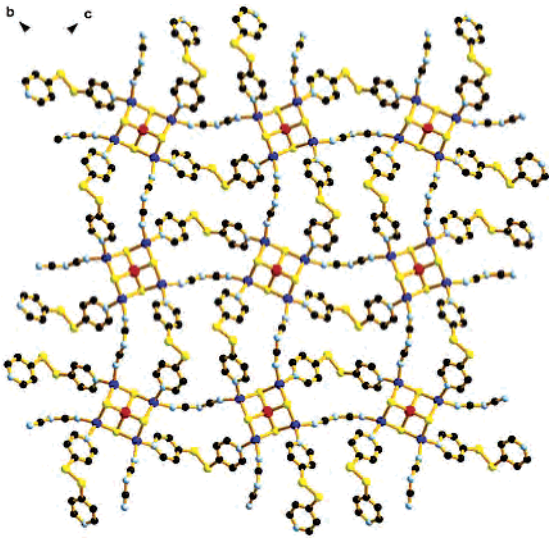

Figure 4. Extended structure of **5** looking down the *a* axis.

Topologically, each $[WS_4Cu_4]$ core in **5** also serves as a 4-connecting node that is similar to that of **4**. The mean deviation from the least-squares plane containing N2, N5, N3B, N1B, N5A, N2A, N3C, and N1C atoms of the four flexible dpds and four dca ligands surrounding the $[WS_4Cu_4]$ core in **5** is ca. 1.17 Å, suggesting that the eight coordination sites of the dpds and dca ligands are approximately locating on a same plane highlighted in gray in Figure 3b. Thus, the $[WS_4Cu_4]$ core in **5** under the presence of the four dpds and four dca ligands may be visualized as another kind of planar 4-connecting node. Each $[WS_4Cu_4]$ core in **5** is interconnected via four pairs of Cu−$\mu_{1,5}$-dca−Cu and Cu−dpds−Cu bridges to form a 2D $[WS_4Cu_4(dca)_2(dpds)_2]_n$ layer network extended along the *bc* plane (Figure 4). The assembled 2D sheet is achiral as the repeating $[WS_4Cu_4]$ core has four dca ligands and four dpds ligands of either the *M*- or *P*-form symmetrically coordinated at four Cu centers. Between the layers are lying the Et_2O and MeCN solvent molecules, and there exists no evident interaction between the layers and the solvated molecules.

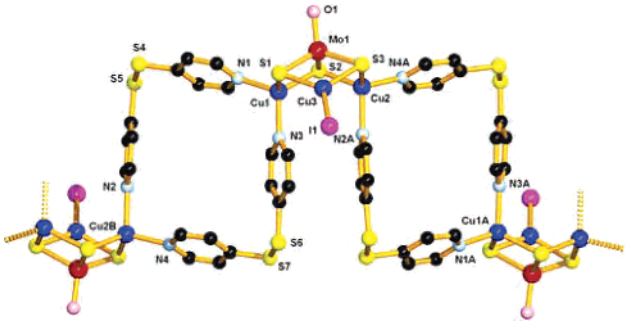

Figure 5. Perspective view of a $[MoOS_3Cu_3I(dpds)_2]$ molecule of **6** with 50% thermal ellipsoids. All hydrogen atoms are omitted for clarity. Symmetry transformations used to generate equivalent atoms: (A) $-x + 1, y - 0.5, -z + 0.5$; (B) $-x + 1, y + 0.5, -z + 0.5$.

Table 4. Selected Bond Distances (Å) and Angles (deg) for **6**

Mo1−O1	1.711(7)	Mo1−S2	2.268(3)
Mo1−S3	2.269(3)	Mo1−S1	2.272(3)
Mo1−Cu3	2.6680(18)	Mo1−Cu1	2.6731(16)
Mo1−Cu2	2.6909(15)	I1−Cu3	2.4608(17)
Cu1−N3	2.044(9)	Cu1−N1	2.084(9)
Cu1−S2	2.263(3)	Cu1−S1	2.290(3)
Cu2−N4A	2.047(9)	Cu2−N2A	2.088(9)
Cu2−S2	2.273(3)	Cu2−S3	2.288(3)
Cu3−S1	2.243(3)	Cu3−S3	2.248(3)
S4−S5	2.028(4)	S6−S7	2.025(5)
O1−Mo1−S2	111.8(3)	O1−Mo1−S3	111.2(3)
S2−Mo1−S3	107.80(10)	O1−Mo1−S1	111.1(3)
S2−Mo1−S1	108.10(10)	S3−Mo1−S1	106.67(11)
Cu3−Mo1−Cu1	86.90(5)	Cu3−Mo1−Cu2	83.28(5)
Cu1−Mo1−Cu2	86.20(5)	N3−Cu1−N1	106.1(4)
N3−Cu1−S2	112.0(3)	N1−Cu1−S2	113.2(3)
N3−Cu1−S1	111.4(3)	N1−Cu1−S1	106.3(3)
S2−Cu1−S1	107.66(10)	N4A−Cu2−N2A	102.3(3)
N4A−Cu2−S2	117.1(3)	N2A−Cu2−S2	110.3(3)
N4A−Cu2−S3	109.1(3)	N2A−Cu2−S3	111.1(3)
S2−Cu2−S3	107.02(10)	S1−Cu3−S3	108.41(11)
S1−Cu3−I1	127.10(10)	S3−Cu3−I1	124.38(9)
Cu3−S1−Mo1	72.42(9)	Cu3−S1−Cu1	108.24(13)
Mo1−S1−Cu1	71.73(9)	Cu1−S2−Mo1	72.31(8)
Cu1−S2−Cu2	107.82(11)	Mo1−S2−Cu2	72.69(8)
Cu3−S3−Mo1	72.40(9)	Cu3−S3−Cu2	103.45(11)
Mo1−S3−Cu2	72.39(9)		

Crystal Structure of $[MoOS_3Cu_3I(dpds)_2]\cdot 0.5DMF\cdot 2(MeCN)_{0.5}$ ($6\cdot 0.5DMF\cdot 2(MeCN)_{0.5}$). Compound $6\cdot 0.5DMF\cdot 2(MeCN)_{0.5}$ crystallized in the monoclinic space group $P2_1/c$, and the asymmetric unit contains one $[MoOS_3Cu_3I(dpds)_2]$ molecule, half of a DMF, and two halves of MeCN-solvated molecules. Figure 5 shows the perspective view of the repeating unit of **6**, and Table 4 presents the selected bond lengths and angles for **6**. The $[MoOS_3Cu_3I(dpds)_2]$ molecule consists of a nido-shaped $[MoOS_3Cu_3]$ core, which closely resembles those in $[MoOS_3Cu_3IL_2]$ (L = 2,2′-bipy,[21a] phen[21b]). The three Cu atoms in **6** show different coordination geometries. Cu1 and Cu2 adopt a distorted tetrahedral coordination geometry, coordinated by two μ_3-S atoms from the $[MoOS_3]^{2-}$ anion and two N atoms from two dpds ligands. Cu3 has an approximate trigonal planar environment, coordinated by one I and two μ_3-S atoms. Because of the different coordination geometries of the three Cu atoms, the Mo1···Cu contacts are different. The mean value for Mo1···Cu1 and Mo1···Cu2 contacts is slightly longer than those of the corresponding ones in $[MoOS_3Cu_3IL_2]$ (2.664(2) Å for L = 2,2′-bipy, 2.638(6) Å for L = phen). The Mo1···Cu3 contact (2.6680(18) Å) is between the corresponding ones of $[MoOS_3Cu_3I(2,2'\text{-bipy})_2]$ (2.640(2) Å) and $[MoOS_3Cu_3I(phen)_2]$ (2.680(6) Å). The various Cu−μ_3-S bond lengths also show the different coordination modes of the three Cu atoms in **6**. For a trigonally coordinated Cu, the average Cu−μ_3-S bond length (2.246(3) Å) is comparable to those of the corresponding ones in $[MoOS_3Cu_3IL_2]$ (2.243(3) Å for L = 2,2′-bipy, 2.252(10) Å for L = phen). For a tetrahedrally coordinated Cu, the mean Cu−μ_3-S bond length (2.279(3) Å) is somewhat longer than those of the corresponding ones in $[MoOS_3Cu_3IL_2]$ (2.252(12) Å for L = 2,2′-bipy, 2.259(10) Å for L = phen). The terminal Cu3−I1 length of 2.4611(17) Å is between that of $[MoOS_3Cu_3I(2,2'\text{-bipy})_2]$ (2.449(2) Å) and that of $[MoOS_3Cu_3I(phen)_2]$ (2.470(9) Å). The mean Cu−N length (2.063(9) Å) is slightly shorter than those in $[MoOS_3Cu_3IL_2]$ (2.081(4) Å for L = 2,2′-bipy, 2.097(23) Å for L = phen). The terminal Mo1−O1 bond length (1.711(7) Å) and the mean bridging Mo1−S distance (2.277(2) Å) in **6** are comparable to the corresponding ones in $[MoOS_3Cu_3IL_2]$ (1.690(3)/2.274(3) Å for L = 2,2′-bipy, 1.691(11)/2.272(8) Å for L = phen). The two dtdp ligands in **6** also basically keep the gauche conformation of the free dtdp ligand. The S−S bond lengths (average 2027(4) Å) are almost the same, while their C−S−S−C dihedral angles are 3.6−5.6° smaller than that of the free dpds ligand.

From a topological perspective, the nido-like $[MoOS_3Cu_3]$ core in **6** may be considered as a 2-connecting node, which is linked to two equivalent cores via two pairs of dpds ligands to form a 1D spiral chain extended along the *b* axis (Figure 6). Each 1D chain is chiral and is represented by either −*M*-$[MoOS_3Cu_3]$−*M*-$[MoOS_3Cu_3]$−*M*-(*M*-chain) or −*P*-$[MoOS_3Cu_3]$−*P*-$[MoOS_3Cu_3]$−*P*-(*P*-chain). This compound consists of a 1:1 ratio of *P*- and *M*-chains and is achiral

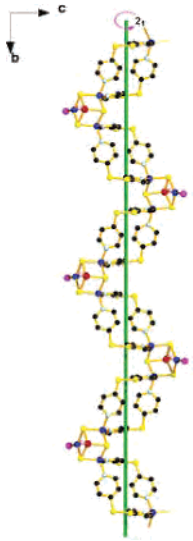

Figure 6. Perspective view of a portion of the 1D spiral chain of **6** extended along the *b* axis.

(21) (a) Zheng, H. G.; Zhang, C.; Chen, Y.; Xin, X. Q.; Leung, N. H. *Synth. React. Inorg. Met.-Org. Chem.* **2000**, *30*, 349. (b) Hou, H. W.; Ang, H. G.; Ang, S. G.; Fan, Y. T.; Low, M. K. M.; Ji, W.; Lee, Y. W. *Inorg. Chim. Acta* **2000**, *299*, 147.

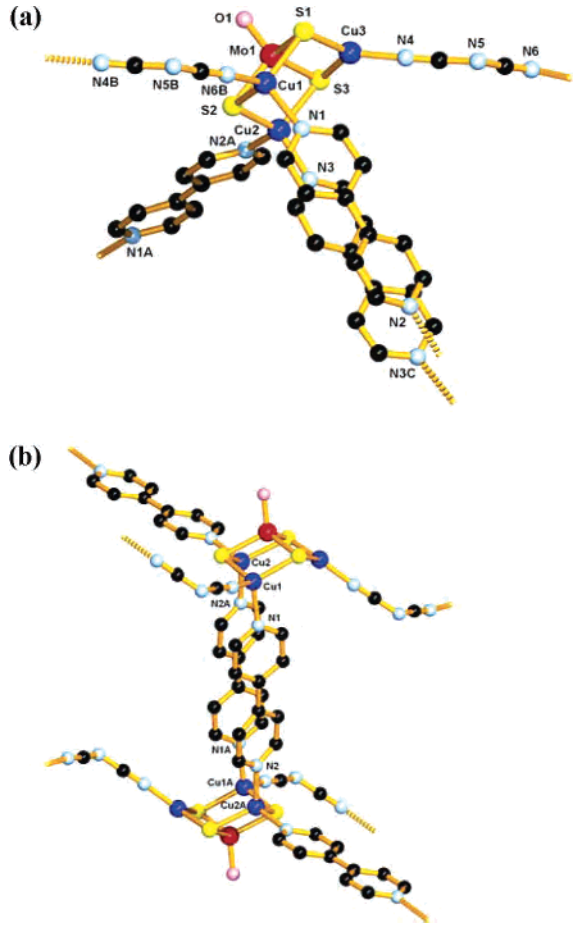

Figure 7. (a) Perspective view of the $[MoOS_3Cu_3(dca)(4,4'\text{-bipy})_{1.5}$ molecule of **7** with 50% thermal ellipsoids. All hydrogen atoms are omitted for clarity. Symmetry transformations used to generate equivalent atoms: (A) $-x + 2, -y + 2, -z + 2$; (B) $x - 1, y - 1, z$; (C) $-x + 2, -y + 1, -z + 2$. (b) Perspective view of the dimeric $\{[MoOS_3Cu_3]_2(dca)_2(4,4'\text{-bipy})_3\}$ species of **7**. All hydrogen atoms are omitted for clarity.

with a centrosymmetric space group $P2_1/c$. The DMF and MeCN solvent molecules are lying between the chains, and no evident interaction is observed between the chain and the solvated molecules. Alternatively, the 1D chain structure may be described as being built of cationic $[Cu(dpds)]_2^{2+}$ squares interconnected by $[MoOS_3(CuI)]^{2-}$ cluster anions via three μ_3-S atoms. There is a 2_1 axis running through the center of each $[Cu(dpds)]_2^{2+}$ square within the chain. The internal cavity for each square has an approximate dimension of 9.77 Å (Cu1···Cu2B separation) × 10.15 Å (S4···S6 separation). In addition, there is a weak $\pi\cdots\pi$ interaction (3.721 Å) between the pyridyl group with N3 and that with N2A.

Crystal Structure of $[MoOS_3Cu_3(dca)(4,4'\text{-bipy})_{1.5}]\cdot$ DMF·MeCN (7·DMF·MeCN). **7**·DMF·MeCN crystallized in the triclinic space group $P\bar{1}$, and the asymmetric unit consists of half of the dimeric $\{[MoOS_3Cu_3]_2(dca)_2(4,4'\text{-bipy})_3\}$ molecule and one DMF and one MeCN solvent molecules. Figure 7 presents the perspective view of the repeating unit of **7**, and Table 5 lists the selected bond lengths and angles for **7**. Two nido-like $[MoOS_3Cu_3]$ cores (Figure 7a) are linked by a pair of parallel 4,4′-bipy bridges to form a centrosymmetrically related $\{[MoOS_3Cu_3]_2(dca)_2(4,4'\text{-bipy})_3\}$ dimer (Figure 7b). The resulting narrow mesh within the dimer is estimated to be a size of 3.5 Å × 11.2 Å. Each $[MoOS_3Cu_3]$ core structure in **7** closely resembles those of **3** and **6**. Of the three copper atoms, Cu3 is three-coordinated by one N from dca anion and two μ_3-S atoms, and the Mo1···Cu3 contact (2.6265(14) Å) is shorter than the corresponding one of **3** (average 2.647(2) Å) and **6**. On the other hand, Cu1 is tetrahedrally coordinated by a N atom (4,4′-bipy), a N (dca) atom, and two μ_3-S atoms while Cu2 is four-coordinated by two N atoms (4,4′-bipy) and two μ_3-S atoms. The mean Mo1···Cu contact (2.6782(12 Å) for Cu1 and Cu2 is somewhat shorter than that of the corresponding ones in **6**. Again, the dca ligands serve as a $\mu_{1,5}$ coordination mode. The tetrahedrally coordinated Cu1−N6B (dca) bond length of 1.970(4) Å is shorter than that of **4**. The Cu3−N4 (dca) bond length of 1.894(4) Å is shorter than that in those containing trigonally coordinated Cu $[(tmpyz)Cu(dca)]_n$ (1.911(2)−1.931(2) Å; tmpyz = 2,3,5,6-tetramethylpyrazine).[18b] The Cu−μ_3-S bond lengths (average 2.249(2) Å for trigonally coordinated Cu and average 2.274(2) Å for tetrahedrally coordinated Cu), Cu−N (4,4′-bipy) distances (average 2.067(6) Å), the terminal Mo1−O1 length (1.724(5) Å), and the bridging Mo1−S distances (average 2.265(2) Å) are normal relative to those of the corresponding ones in **6**.

Table 5. Selected Bond Distances (Å) and Angles (deg) for **7**

Mo1−O1	1.724(5)	Mo1−S2	2.2555(18)
Mo1−S1	2.2672(18)	Mo1−S3	2.2710(18)
Mo1−Cu3	2.6265(14)	Mo1−Cu2	2.6582(12)
Mo1−Cu1	2.6981(12)	Cu1−N6D	1.970(6)
Cu1−N1	2.100(6)	Cu1−S1	2.2701(19)
Cu1−S2	2.2867(19)	Cu2−N2A	2.025(6)
Cu2−N3	2.075(6)	Cu2−S2	2.269(2)
Cu2−S3	2.2711(19)	Cu3−N4	1.894(6)
Cu3−S3	2.2467(19)	Cu3−S1	2.250(2)
N2−Cu2A	2.025(6)	N6−Cu1E	1.970(6)
O1−Mo1−S2	111.13(16)	O1−Mo1−S1	111.07(16)
S2−Mo1−S1	107.64(7)	O1−Mo1−S3	110.39(16)
S2−Mo1−S3	108.41(7)	S1−Mo1−S3	108.07(7)
Cu3−Mo1−Cu2	89.60(4)	Cu3−Mo1−Cu1	88.15(4)
Cu2−Mo1−Cu1	87.37(4)	N6D−Cu1−N1	103.6(2)
N6D−Cu1−S1	118.81(19)	N1−Cu1−S1	110.08(17)
N6D−Cu1−S2	110.65(18)	N1−Cu1−S2	106.68(17)
S1−Cu1−S2	106.48(7)	N2A−Cu2−N3	99.0(2)
N2A−Cu2−S2	120.45(18)	N3−Cu2−S2	105.02(16)
N2A−Cu2−S3	113.19(18)	N3−Cu2−S3	110.30(16)
S2−Cu2−S3	107.96(7)	N4−Cu3−S3	124.10(19)
N4−Cu3−S1	124.90(19)	S3−Cu3−S1	109.55(7)
Cu3−S1−Mo1	71.11(6)	Cu3−S1−Cu1	110.08(8)
Mo1−S1−Cu1	72.98(6)	Mo1−S2−Cu2	71.97(6)
Mo1−S2−Cu1	72.88(6)	Cu2−S2−Cu1	108.61(8)
Cu3−S3−Mo1	71.09(6)	Cu3−S3−Cu2	111.02(8)
Mo1−S3−Cu2	71.64(6)		

Topologically, each $[MoOS_3Cu_3]$ core in **7** serves a rare seesaw-shaped 4-connecting node and is linked by a pair of dca anions at Cu1 and Cu3 to form a 1D $[MoOS_3Cu_3(dca)]_n$ chain extended along the *a* axis. Such a chain and its centrosymmetrically related one are then bridged by a pair of parallel 4,4′-bipy ligands to form a 1D $\{[MoOS_3Cu_3(4,4'\text{-bipy})]_2(dca)_2\}_n$ double chain where the orientation of the $[MoOS_3Cu_3]$ core is alternating. Each resulting double chain is further interconnected by another pair of symmetry-related 4,4′-bipy ligands to form a unique 2D staircase network extended along the *ab* plane (Figure 8). The layers are squeezed with DMF- and MeCN-solvated molecules, and

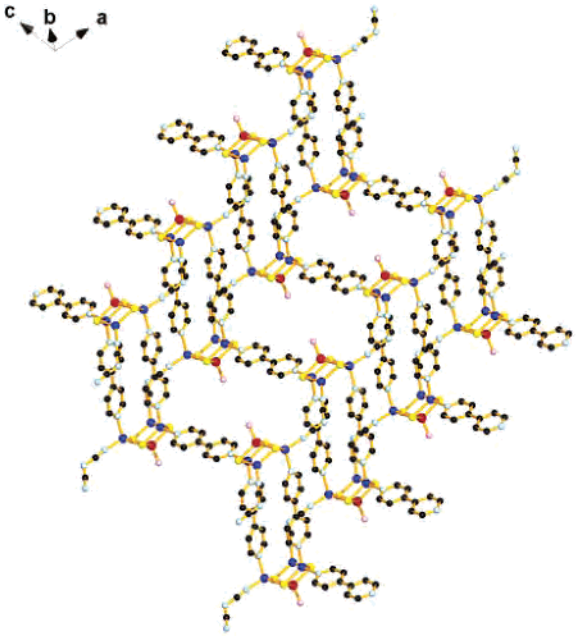

Figure 8. Extended structure of **7** looking down the *c* axis. All hydrogen atoms are omitted for clarity.

no evident interactions between layers and the solvent molecules exist.

Concluding Remarks

In this paper, we demonstrated new approaches to the construction of new 1D or 2D $[WS_4Cu_4]$- or $[MoOS_3Cu_3]$-based supramolecular arrays **4**−**7** from reactions of the preformed clusters **1**−**3** with flexible ditopic linkers such as dps, dpds, and their combinations with dca and 4,4′-bipy. In these compounds, either $[WS_4Cu_4]$ core in **1** or $[MoOS_3Cu_3]$ core in **2** and **3** was retained and served as interesting multiconnecting nodes. Both **4** and **5** consist of a 2D array in which each saddle-shaped $[WS_4Cu_4]$ core, serving a planar 4-connecting node, interconnects with other four equivalent cores via six dps liands or four pairs of dca and dpds ligands. Compound **6** exhibits a 1D spiral chain of the nido-like $[MoOS_3Cu_3I]$ species linked by two pairs of dpds ligands. Compound **7** shows a 2D staircase net in which each $[MoOS_3Cu_3]$ core, acting as a seesaw-shaped 4-connecting node, is interlinked by a pair of dca anions and three 4,4′-bipy ligands to other four equivalent cores. To the best of our knowledge, **4** (or **5**) and **7** represent the first examples that hold a planar or a seesaw-shaped 4-connecting node in the cluster-based supramolecular chemistry. These interesting topological structures of **4**−**7** coupled with the 3D porous polymer reported previously[17b] make **1**−**3** very promising precursors for the rational design and construction of cluster-based supramolecular compounds. We are currently extending this work by investigation into the assembly of new $[WS_4Cu_4]$- or $[MoOS_3Cu_3]$-based supramolecular architectures from reactions of **1**−**3** with other flexible multitopic ligands such as dpm (1,1′-dipyridylmethane), dpe (1,2-dipyridylethane), etc.

Acknowledgment. This work was financially supported by the NNSF (Grants 20271036 and 20525101), the NSF of Jiangsu Province (Grant BK2004205), the Specialized Research Fund for the Doctoral Program of Higher Education (Grant 20050285004), the Qin-Lan Project of Jiangsu Province, the State Key Laboratory of Organometallic Chemistry of Shanghai Institute of Organic Chemistry (Grant 06-26), and the Scientific Research Foundation for the Returned Overseas Chinese Scholars, State Education Ministry of China. We highly appreciated useful suggestions from the Editor and the reviewers.

Supporting Information Available: Crystallographic data for compounds **4**·2MeCN, **5**·Et_2O·2MeCN, **6**·0.5DMF·2$(MeCN)_{0.5}$, and **7**·DMF·MeCN (CIF) and the synthesis and characterization of the brown-red solid $[WS_4Cu_4(dca)_2]$ (in PDF format). This material is available free of charge via the Internet at http://pubs.acs.org.

IC060974D